Unfolding the relation between global temperature and ENSO

A. A. Tsonis,[1] J. B. Elsner,[2] A. G. Hunt,[3] and T. H. Jagger[2]

Received 1 March 2005; revised 25 March 2005; accepted 30 March 2005; published 3 May 2005.

[1] An analysis of global temperature and ENSO data indicates that their relationship is more complicated than currently thought. Indeed, it appears that there are two complimenting aspects to this relation. The first (and known) aspect expresses the fact that global temperature increases after an El Nino event and a La Nina event follows an El Nino event. Thus, El Nino forces global temperature. While this is an important result, it is not the entire picture. If it were, ENSO would be independent of global temperature. The second aspect, which is proposed here, suggests a deeper connection between global temperature and ENSO. We find that ENSO is not independent and that positive (negative) global temperature tendency tends to trigger an El Nino (La Nina). Thus, in a warming climate El Nino events will be more frequent than La Nina events. The methodology presented in this paper may elucidate how realistically coupled ocean-atmosphere models simulate the response of climate to global change. **Citation:** Tsonis, A. A., J. B. Elsner, A. G. Hunt, and T. H. Jagger (2005), Unfolding the relation between global temperature and ENSO, *Geophys. Res. Lett.*, *32*, L09701, doi:10.1029/2005GL022875.

1. Introduction

[2] Under normal conditions the westward equatorial trade winds of the tropical Pacific force equatorial Rossby waves, which pile up warm surface water toward the west. This deepens the equatorial thermocline in the west creating a thermal reservoir and raises it in the east causing upwelling of cold water to the surface in the east. Warming in the west and cooling in the east is enhanced during a La Nina event. A weakening or reversal of the trade winds (through anomalous westerly wind bursts) initiates Kelvin waves, which travel eastward and which reduce the upwelling thereby diminishing the thermal contrast between west and east. At the same time the warm surface water above the thermocline sloshes back and spreads to the east producing a large area of warm surface water in the eastern Pacific Ocean called an El Nino event. During both events increased convection over the warm surface provides a positive feedback mechanism that leads to either enhanced trade winds (during La Nina) or anomalous westerly winds (during El Nino). While the build up of heat content in the west may set the stage for the development of an El Nino, ENSO is often modulated by higher frequency variability. This variability may arise from the Madden-Julian Oscillation (MJO) [*Madden and Julian*, 1972], which produces westerly wind events, which in turn can generate Kelvin waves as they propagate eastward [*McPhaden*, 1999]. Kelvin waves can also be generated by Rossby waves reflecting at the western boundary. These Kelvin waves take a few months to traverse the Pacific introducing a time lag between the trigger and surface warming in the east. The net result is a complex aperiodic phenomenon.

[3] The processes described above comprise modern theories and models of ENSO evolution [*Battisti*, 1988; *Schopf and Suarez*, 1987; *Suarez and Schopf*, 1988; *Zebiak and Cane*, 1987; *Neelin et al.*, 1998; *Blanke et al.*, 1997; *Fedorov*, 2002; *Penland and Matrosova*, 1994]. These theories and models, however, have yet to explain the fine details behind the initiation of an event and the role global change plays. For example, what is the origin of the anomalous wind bursts? Why in the period 1976–1998 has there been several strong El Nino events and hardly any La Nina events? Why do the models not respond the same way as global temperature changes [*Timmermann et al.*, 1999; *Collins*, 2000; *Collins et al.*, 2005]? This paper examines the relationship of global temperature and ENSO and offers some answers to the above questions.

2. Data Analysis and Results

[4] We begin by considering the cross-correlation between global temperature, T, and the Southern Oscillation Index (SOI) where the temperatures are from the detrended Intergovernmental Panel for Climate Change (IPCC) record. In order to make direct connections between higher (lower) temperatures and El Nino (La Nina) frequency of occurrence we reverse the SOI sign so that positive values indicate El Nino and negative values indicate La Nina. We observe (Figure 1a) that the cross-correlation structure is characterized on the average by positive correlations for positive lags (when SOI leads T). This indicates that El Ninos precede higher global temperatures and La Ninas precede lower global temperatures. At the same time we observe a general tendency for negative correlations for negative lags (when T leads SOI). This indicates that lower global temperatures precede El Nino events and higher global temperatures precede La Nina events. Similar results are obtained when instead of SOI we use the N3.4 index (Figure 1b). Thus, Figure 1 displays the well-known result that El Nino tends to increase the average temperature of the planet and that in general a La Nina succeeds an El Nino. Mechanisms for this warmth can be traced to changes in cloudiness and atmospheric circulations [*Trenberth et al.*, 2002; *Klein et al.*, 1999; *Kumar and Hoerling*, 2003]. Next, we present results that add another piece to the puzzle of the relationship between ENSO and global temperature.

[1]Atmospheric Sciences Group, Department of Mathematical Sciences, University of Wisconsin-Milwaukee, Milwaukee, Wisconsin, USA.
[2]Department of Geography, Florida State University, Tallahassee, Florida, USA.
[3]Department of Physics, Wright State University, Dayton, Ohio, USA.

0094-8276/05/2005GL022875$05.00

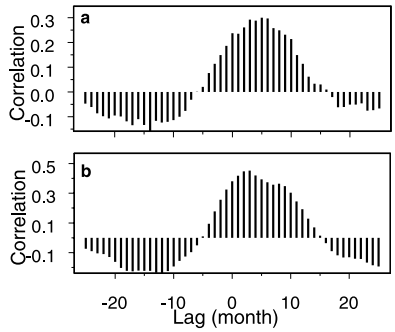

Figure 1. (a) Time domain analysis of global temperature and ENSO. This graph shows the cross-correlation between global temperature and negative values of the SOI based on 1248 consecutive months from 1900–2003. The overall trend in the global temperature is removed. (b) Same as Figure 1a but when the N3.4 index is used instead of SOI. The values of N3.4 are based on data from 1950–2003. N3.4 is the average sea surface temperature in the box 5°N–5°S, 170°W–120°W.

[5] Figure 2a shows the cross-correlation between SOI and the $\Delta T/\Delta t$ function (for Δt = 1 month) for positive lags (SOI leads ΔT) and for negative lags (ΔT leads SOI). Two important points come out of this analysis. First, there is a peak at about lag = −5 months with positive correlations and a peak at about lag = +11 months with negative correlations. This overall variation of the cross-correlation indicates a 30–40 month coherency. Superimposed on this cycle is a high frequency oscillation of about three months. Because the correlations are not large, we test the statistical significance of these two oscillations in the cross-correlation function using coherency analysis in the frequency domain. Figure 2b shows the squared coherency between global temperature and SOI. Coherence measures the linear dependence of the oscillatory components in the two detrended signals. While it does not indicate cause and effect, significant coherence suggests that changes in one signal relate to changes in the other signal. When the squared coherency is transformed by the inverse hyperbolic tangent, the resulting values have a normal distribution centered on zero and with a variance proportional to the sum of squares of the smoothing weights [*Kuo et al.*, 1990]. This allows us to make a correspondence between the values of squared coherency and confidence levels. For example, for a given frequency, squared coherency values of 0.2 and 0.25 define the approximate 90% and 95% confidence levels, respectively, for incoherent series. Accordingly, Figure 1b indicates that the coherence between temporal changes in T and SOI is high in the frequency band centered at about 0.32 cycles/month and exceptionally high in the frequency band centered at about 0.028 cycles/month. These statistically significant coherency bands correspond to time scales of three and 36 months observed in the time analysis and are similar to the time scales of Kelvin waves and the El Nino/La Nina cycle, respectively. It thus appears that processes associated with these two major time scales largely determine the cross-correlation structure between changes in global temperature and SOI. This agrees well with the evolution of ENSO discussed above. Phase estimates of the coherence (not shown) indicate that in the high frequency coherent band, temperature fluctuations lead SOI by about three months. Since this band is in the Kelvin wave scale, this implies that temperature fluctuations may precede Kelvin wave formation. Since Kelvin wave formation is due to a westerly wind stress anomaly, it follows that anomalous westerly wind bursts may be modulated by global temperature changes. This is an important finding as it ties global temperature fluctuations directly to the emergence of the anomalous wind bursts and thus in the triggering of El Nino.

[6] Second, the positive correlations in Figure 2a when ΔT leads SOI indicate that positive (negative) temperature fluctuations precede El Nino (La Nina) development. At the same time, the negative correlations when SOI leads ΔT indicate that El Nino (La Nina) relate to future negative (positive) temperature tendencies. This suggests that a positive (negative) global temperature tendency triggers an El Nino (La Nina), which ultimately reverses the tendency. True enough (as we show in Figure 1) once an El Nino is initiated and warm water spreads over a significant portion of the planet, the global mean temperature will increase (also as mentioned above other mechanisms contribute to this warming). Thus, initially the role of El Nino is to support the positive tendency. Note that the contribution of ENSO to the long-term temperature trend in the last 50 years is about 0.06°C or 10% of the overall trend [*Trenberth et al.*, 2002]. However, as Figure 2a indicates, after a time scale of the order of 16 (5 + 11) months, El Nino's role is to reverse that tendency. This is in agreement with others who have observed that it takes 16–18 months for El Nino to deplete the storage of heat in the west part of the Pacific basin [*Neelin et al.*, 1998]. After El Niño has run its course, the stored heat in the equatorial and off-equatorial Pacific is eliminated as it disperses in the atmosphere and is transported poleward by ocean currents to be incorporated in the

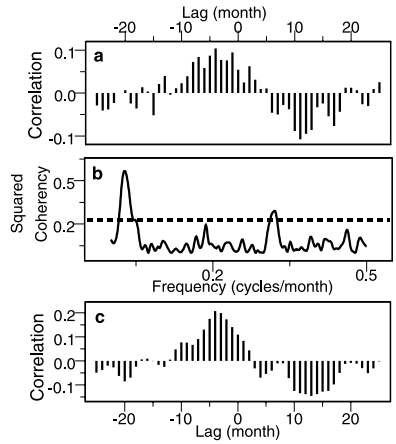

Figure 2. Time and frequency domain analysis of global temperature tendency and ENSO. (a) Cross-correlations of temperature tendency and negative values of the SOI. (b) Square coherency between global temperature and SOI. The broken horizontal line indicates the approximate 90% significance level. The squared coherency is smoothed using a "Daniell" window and a taper of 0.1. (c) Same as Figure 2a but when the N3.4 values are used instead of the SOI values.

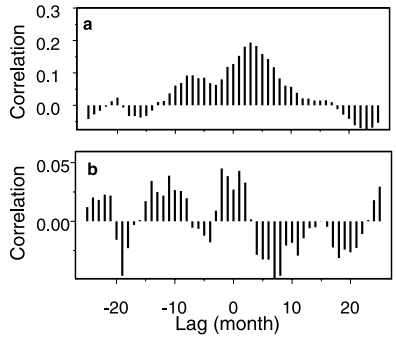

Figure 3. (a) Same as Figure 1b but using global temperature and ENSO data from a 119-year CSM simulation. (b) Same as Figure 2c but using data from a 119-year CSM simulation.

formation of mid-latitude storms [*Wang et al.*, 2003; *Lau et al.*, 2004; *Sun and Trenberth*, 1998]. This leads to a reduction in atmospheric temperatures as heat is again deposited in the thermal reservoir in the western Pacific. Analogous arguments hold for La Nina. This result is in agreement with previous work investigating scaling properties of global temperature records that show a change from persistence (Hurst exponent > 1/2) to self-correction (Hurst exponent < 1/2) [*Tsonis et al.*, 1998] at time scales relevant to ENSO. Similar results hold when the Nino 3.4 (N3.4) index is used instead of the SOI (Figure 2c). The idea that ENSO acts as a 'safety valve' in the climate system is consistent with the 'heat pump' hypothesis for ENSO, which states that ENSO helps to shed excess heat in the tropics [*Sun and Trenberth*, 1998; *Sun*, 2000].

[7] The physics behind the above results is complex but well understood. An increase in global temperature leads to a rapid (and greater) heat storage in the tropical Pacific [*Latif et al.*, 1997]. Increased heat storage leads to stronger trade winds [*Latif et al.*, 1997; *Shriver and O'Brien*, 1995]. Scaling arguments for turbulent flow in boundary layers as well as thermodynamic arguments dictate that an increase in trade wind strength induces an increase in trade wind fluctuations [*Kolmogorov*, 1941]. If this were not true the system must have negative absolute temperatures. These wind fluctuations, however, will not trigger El Ninos and La Ninas with equal chance. With rapid storage of energy the thermal and physical inertia of the regions of heat storage in the western Pacific increase more rapidly, with a tendency for enhanced sea surface elevation gradients. These gradients suppress the triggering of La Nina, even when the trade winds are stronger and fluctuations are larger. Thus, when global temperatures are on the rise, El Nino is favored over La Nina. A corollary of the above is that in a scenario of a sustained positive (negative) global temperature tendency (which will result in a positive (negative) long-term trend), the frequency of El Nino events will be greater (less) than that of La Nina events. Recent observations support this conclusion. In the period 1976–1998 the globe experienced a pronounced positive temperature trend and several strong El Nino events but hardly any La Nina events. The same is true for the period of rising temperatures at the beginning of the 20th century (1900–1925) when El Nino events were more frequent. In contrast during the period 1925–1975 when no marked positive or negative temperature trend was observed, El Nino and La Nina occurred with similar frequency. Note that the results agree with the theory on the relation between global change and ENSO recently proposed by *Tsonis et al.* [2003]. It follows that this second aspect in the relation between global temperature and ENSO is backed by physical mechanisms and it is consistent with the observed frequency of El Nino and La Nina and with previous work. Note that we are not claiming that there will be more El Nino events with a warmer planet (an issue which is still open), but rather more El Nino events with a *warming* planet.

[8] We thus see that there are two aspects in the relation between global temperature and ENSO. The first is the well-known result that El Nino tends to increase the average temperature of the planet. The second aspect is more complex as it indicates that global temperature fluctuations provide the triggering mechanism and that once an event is triggered it eventually acts to reverse the sign of the fluctuation. These two aspects form a negative feedback loop which controls runaway tendencies.

3. A Test for Models

[9] As was mentioned above coupled ocean/atmosphere GCMs do not universally agree on how they respond to a warmer global temperature. The method presented here can be used on model simulations to verify whether or not a model realistically simulates the ENSO cycle. If a model simulation reproduces to a good degree the two aspects of the relation between global temperature and ENSO, then the model simulates the cycle realistically. As an example we test NCAR's Climate System Model 1 (CSM1). We use the output of a 119-year experiment in which the global temperature is forced to increase by a rising CO_2 concentration rate of 1%/year from its pre-industrial level (case b006, data accessible at www.ucar.edu). First we compute the monthly mean surface global and N3.4 temperature. Then we remove the annual cycle by computing monthly anomalies and repeat the above correlation/coherence analysis. Although the correlations are generally smaller, the results from this model are qualitatively similar to those in Figures 1 and 2. Figure 3a is similar to Figure 1b and Figure 3b to Figure 2c but using the model output. By comparing 3a and 1b we find that the cross-correlation functions have the same sign in 39 out of 51 lags. From Figures 3b and 2c we find that that the cross-correlation functions have the same sign in 35 out of 51 lags. Thus, this model simulation agrees with the observed cross-correlation function between T and N3.4 in 76% of the lags and with the observed cross-correlation function between ΔT and N3.4 in 68% of the lags.

[10] Moreover, this model output confirms the corollary that in a scenario of a sustained positive (negative) global temperature tendency, the frequency of El Nino events will be greater (less) than that of La Nina events. In this 120-year simulation, the El Nino frequency is 20/century, while the La Nina frequency is 11/century. On the contrary, in a 300-year steady state experiment with the same model (case b003), El Nino and La Nina events occur at roughly the same frequency (about 17 events/century). Here an event is defined as greater than a one standard deviation

from the mean N3.4 index, which persists at least 6 months (positive departures for El Nino). Even though not perfectly, this model appears to capture qualitatively and quantitatively both aspects of the observed relation between global temperature and ENSO.

4. Conclusions

[11] We present evidence that establishes a clearer picture of how global change relates to ENSO variability. The most important result is that positive temperature fluctuations tend to trigger an El Nino and negative fluctuations tend to trigger a La Nina; a result that provides an observational target for coupled ocean-atmosphere models. This result is supported by physical arguments, observations, past work and model simulations. It follows, that in a warming climate the frequency of El Nino events will be greater than the frequency of La Nina events. This makes global temperature change (which can be either the result of natural variability and/or the result of anthropogenic effects) an important input to ENSO dynamics. Since ENSO effects are worldwide, this makes predictions of global temperature trends of paramount importance in forecasting changes in weather patterns in the 21st century.

[12] **Acknowledgment.** We thank Kyle Swanson for help with the CSM data.

References

Battisti, D. S. (1988), Dynamics and thermodynamics of a warming event in a coupled tropical atmosphere-ocean model, *J. Atmos. Sci.*, *45*, 2889–2919.

Blanke, B., J. D. Neelin, and D. Gutzler (1997), Estimating the effect of stochastic wind forcing on ENSO irregularity, *J. Clim.*, *10*, 1473–1486.

Collins, M. (2000), The El Nino–Southern Oscillation in the second Hadley Centre coupled model and its response to greenhouse warming, *J. Clim.*, *13*, 1299–1312.

Collins, M., and the CMIP Modeling Groups (2005), El Nino- or La Nina-like climate change?, *Clim. Dyn.*, in press.

Fedorov, A. V. (2002), The response of the coupled tropical ocean-atmosphere to westerly wind bursts, *Q. J. R. Meteorol. Soc.*, *128*, 1–23.

Kolmogorov, A. N. (1941), Dissipation of energy in locally isotropic turbulence, *Dokl. Akad. Nauk SSSR*, *32*, 16–18.

Klein, S. A., B. J. Soden, and N.-C. Lau (1999), Remote sea surface temperature variations during ENSO: Evidence for a tropical atmospheric bridge, *J. Clim.*, *12*, 917–932.

Kumar, A., and M. P. Hoerling (2003), The nature and causes for the delayed atmospheric response to El Nino, *J. Clim.*, *16*, 1391–1403.

Kuo, C., C. Lindeberg, and D. J. Thomson (1990), Coherence established between atmospheric carbon dioxide and global temperature, *Nature*, *343*, 709–714.

Latif, M., R. Kleeman, and C. Eckert (1997), Greenhouse warming, decadal variability or El Niño? An attempt to understand the anomalous 1990's, *J. Clim.*, *10*, 2221–2239.

Lau, K. M., J. Y. Lee, K. M. Kim, and I. S. Kang (2004), The North Pacific as a regulator of summertime climate over Eurasia and North America, *J. Clim.*, *17*, 819–833.

Madden, R. A., and P. R. Julian (1972), Description of global scale circulation cells in the tropics with 40–50 day period, *J. Atmos. Sci.*, *29*, 1109–1123.

McPhaden, M. J. (1999), Genesis and evolution of the 1997–98 El Nino, *Science*, *283*, 950–954.

Neelin, J. D., D. S. Battisti, A. C. Hirst, and F.-F. Jin (1998), ENSO theories, *J. Geophys. Res.*, *103*, 14,261–14,290.

Penland, C., and L. Matrosova (1994), A balance condition for numerical models with applications to El Nino–Southern Oscillation, *J. Clim.*, *7*, 1352–1372.

Schopf, P. S., and M. J. Suarez (1987), Vacillations in a coupled ocean-atmosphere model, *J. Atmos. Sci.*, *45*, 549–566.

Shriver, J. F., and J. J. O'Brien (1995), Low frequency variability of the equatorial Pacific Ocean using a new pseudostress dataset: 1930–1989, *J. Clim.*, *8*, 2762–2786.

Suarez, M. J., and P. S. Schopf (1988), A delayed action oscillator for ENSO, *J. Atmos. Sci.*, *45*, 3283–3287.

Sun, D.-Z. (2000), The heat sources and sinks of the 1986–87 El Niño, *J. Clim.*, *13*, 3533–3550.

Sun, D.-Z., and K. Trenberth (1998), Coordinated heat removal from the equatorial Pacific during the 1986–87 El Nino, *Geophys. Res. Lett.*, *25*, 2659–2662.

Timmermann, A., et al. (1999), Increased El Niño frequency in a climate model forced by future greenhouse warming, *Nature*, *398*, 694–696.

Trenberth, K. E., J. M. Caron, D. P. Stepaniak, and S. Worley (2002), Evolution of El Niño–Southern Oscillation and global atmospheric surface temperatures, *J. Geophys. Res.*, *107*(D8), 4065, doi:10.1029/2000JD000298.

Tsonis, A. A., P. J. Roebber, and J. B. Elsner (1998), A characteristic time scale in the global temperature record, *Geophys. Res. Lett.*, *25*, 2821–2823.

Tsonis, A. A., A. G. Hunt, and J. B. Elsner (2003), On the relation between ENSO and global climate change, *Meteorol. Atmos. Phys.*, *84*, 229–242.

Wang, X. C., F. F. Jin, and Y. Q. Wan (2003), A tropical ocean recharge mechanism for climate variability. Part I: Equatorial heat content changes induced by the off-equatorial wind, *J. Clim.*, *16*, 3585–3598.

Zebiak, S. E., and M. A. Cane (1987), A model El Nino/Southern Oscillation, *Mon. Weather Rev.*, *115*, 2262–2278.

J. B. Elsner and T. H. Jagger, Department of Geography, Florida State University, Tallahassee, FL 32306, USA.

A. G. Hunt, Department of Physics, Wright State University, Dayton, OH 45435, USA.

A. A. Tsonis, Atmospheric Sciences Group, Department of Mathematical Sciences, University of Wisconsin-Milwaukee, Milwaukee, WI 43201-0413, USA. (aatsonis@uwm.edu)